

Single-cell mapping of regenerative and fibrotic healing responses after musculoskeletal injury

Robert J. Tower,^{1,*} Alec C. Bancroft,¹ Ashish R. Chowdary,¹ Spencer Barnes,^{1,2} Nicole J. Edwards,³ Chase A. Pagani,¹ Lindsay A. Dawson,⁴ and Benjamin Levi^{1,*}

¹Center for Organogenesis and Trauma, Department of Surgery, University of Texas Southwestern Medical Center, Dallas, TX 75390, USA

²Bioinformatics Core, University of Texas Southwestern Medical Center, Dallas, TX 75390, USA

³Department of Surgery, University of Michigan, Ann Arbor, MI 48109, USA

⁴Department of Veterinary Physiology and Pharmacology, Texas A&M University, College Station, TX 77843, USA

*Correspondence: robert.tower@utsouthwestern.edu (R.J.T.), benjamin.levi@utsouthwestern.edu (B.L.)

<https://doi.org/10.1016/j.stemcr.2022.08.011>

SUMMARY

After injury, a cascade of events repairs the damaged tissue, including expansion and differentiation of the progenitor pool and redeposition of matrix. To guide future wound regeneration strategies, we compared single-cell sequencing of regenerative (third phalangeal element [P3]) and fibrotic (second phalangeal element [P2]) digit tip amputation (DTA) models as well as traumatic heterotopic ossification (HO; aberrant). Analyses point to a common initial response to injury, including expansion of progenitors, redeposition of matrix, and activation of transforming growth factor β (TGF- β) and WNT pathways. Surprisingly, fibrotic P2 DTA showed greater transcriptional similarity to HO than to regenerative P3 DTA, suggesting that gene expression more strongly correlates with healing outcome than with injury type or cell origin. Differential analysis and immunostaining revealed altered activation of inflammatory pathways, such as the complement pathway, in the progenitor cells. These data suggests that common pathways are activated in response to damage but are fine tuned within each injury. Modulating these pathways may shift the balance toward regenerative outcomes.

INTRODUCTION

After trauma, healing mechanisms are engaged to restore tissue to its pre-injury condition. The early response to trauma commonly involves restricted blood flow, leading to hypoxia, loss of neural and lymphatic networks, activation of cell stress responses, and apoptosis in cells unable to survive this initial insult (Baker et al., 2018). This stage is typically followed by inflammation, including accumulation of macrophages and T cells, which clear cellular debris. Progenitors in the injured tissue then expand through proliferation (Meyers et al., 2019; Roberts et al., 2015) or dedifferentiation of mature cells (Sousa et al., 2011; Neff 2018; Tanaka et al., 2016). This expanded progenitor pool then undergoes matrix deposition to replace the injured tissue. Depending on the type and location of injury and the means through which this repair is conducted, this repair process can lead to regenerative healing or fibrosis, in which aberrant healing leads to altered cellular and mechanical properties.

Many amphibians and fish have an incredible ability to regenerate complex tissues and even entire limbs, such as regeneration after tail amputation in frog tadpoles (*Xenopus tropicalis*) (Beck et al., 2003, 2009; Kakebeen et al., 2020; Aztekin et al., 2019) and full limb amputation in the axolotl (*Ambystoma mexicanum*) (Gerber et al., 2018; Nacu and Tanaka 2011). In comparison, regeneration in humans is severely restricted (Douglas 1972; Illingworth 1974). In mice, regeneration is restricted to the distal third

of the third phalangeal element (P3), resulting in regeneration of the injured tissue, including formation of new bone, skin, and connective tissue (Han et al., 2008; Simkin et al., 2013; Neufeld and Zhao 1995; Johnston et al., 2016). Across species, regeneration is mediated through formation of a structure known as the blastema, a heterogeneous mass of lineage-restricted fibroblast-like cells (Lehoczy et al. 2011; Johnson et al., 2020). Although the outcome of *de novo* regeneration is similar to early stages of tissue development, the genetic and molecular mechanisms responsible for regeneration remain distinct from that of limb development, even in animals capable of complete regeneration of complex tissues (Gerber et al., 2018; Storer et al., 2020).

Fibrotic healing is another mechanism through which damaged tissue is repaired. However, unlike normal regeneration, in which damaged tissue is replaced with near approximations of their predecessors, fibrotic healing results in abnormal extracellular matrix (ECM) and cell/tissue types. In the case of mouse digit tip amputation (DTA), fibrotic healing is observed when amputation occurs at the second phalangeal element (P2) rather than P3. After P2 DTA, bone heals through endochondral ossification, or mineralization via a cartilage intermediate, in contrast to P3 DTA, which regenerates bone through direct intramembranous ossification. P2 DTA results in capping of the wound with connective tissue, preventing further replacement of the amputated digit (Dawson et al., 2017).





Under more extreme conditions, progenitor cells mobilized for repair after injury undergo abnormal differentiation. Such is the case in traumatic heterotopic ossification (HO). In humans and mouse models, a combined injury- and systemic inflammatory-inducing event (e.g., burn) results in abnormal differentiation of mesenchymal progenitor cells (MPCs) to osteoblasts, resulting in formation of osteoid in the surrounding soft tissue. In mice, this can be accomplished through transection of the Achilles tendon plus an additional burn to the back of the mice (burn/tenotomy [BT]). The result is not only failure to repair the injured tendon but also formation of HO along the tendon ends as well as outgrowths from neighboring bone. Similar to P2 DTA, HO is formed through a cartilage intermediate and has been proposed to occur through differentiation of tendon progenitor cells into chondrocytes (Agarwal et al., 2016). Although the exact mechanism driving this aberrant differentiation remains unknown, interactions with inflammatory cells (Sorkin et al., 2020), as well as mechanical stimuli (Huber et al., 2020; Dolan et al., 2021) have been proposed to regulate the injury response in models of regenerative and fibrotic healing.

Although the overall outcomes are different between HO, P2 DTA, and P3 DTA, the overall processes have several similarities. In mouse P2 and P3 DTA, the blastema is derived from, and largely comprised of, *Pdgfra*-expressing fibroblast-like cells (Johnston et al., 2016; Storer et al., 2020; Carr et al., 2019). Formation of HO after BT has similarly been attributed to *Pdgfra*⁺ progenitors (Agarwal et al., 2016). Cumulatively referred to as MPCs for simplicity, these *Pdgfra*⁺ cells have been shown to be beneficial and detrimental in various models of wound healing, suggesting that their response and differentiation may be influenced by intrinsic differences among MPCs in different locations as well as by differences in their microenvironments. For example, *Pdgfra*⁺ MPCs in skeletal muscle have been shown to support muscle stem cell expansion to facilitate myogenesis (Joe et al., 2010; Wosczyzna et al., 2019). However, resident *Pdgfra*⁺ cells also contribute to fatty infiltration and/or fibrosis after skeletal muscle injury, including in Duchenne muscular dystrophy (Uezumi et al. 2010, 2011; Olson and Soriano 2009) as well as liver fibrosis (Kikuchi and Monga 2015; Kikuchi et al., 2020). In this study, we analyzed the initial injury response, MPC differentiation characteristics, and inflammatory cell interaction between regenerative and fibrotic healing models. Understanding the factors guiding these divergent healing outcomes could prove instrumental for finding new therapeutic strategies to promote tissue regeneration.

RESULTS

Progenitor cells and their lineage descendants show a similar pattern of early transcriptional response to Achilles tendon and digit tip injury

To assess the early injury response, mesenchymal cells (MPCs and their differentiated cell descendants, such as chondrocytes, osteoblasts, and tenocytes) derived from the Achilles tendon at various time points after BT (Sorkin et al., 2020; Pagani et al., 2021; Figure S1A) were subjected to trajectory analysis and placed along a pseudotemporal axis with the root assigned at the earliest stage after injury (Figure 1A). Pseudotime position cells isolated at each time point after injury were quantified relative to values obtained from a healthy, uninjured tendon (Figure 1B). Similar analyses were conducted on fibroblast-like cells and their differentiated descendants (Figures S1B and S1C) derived from the regenerative P3 DTA (Figures 1C and 1D) and fibrotic P2 DTA (Storer et al., 2020; Figures 1E and 1F) injuries. In comparison with HO, both DTA models showed a more uniform transcriptional response to injury, signified by a reduced distribution of fibroblast-like cells derived shortly after injury along the pseudotime axis. To compare overall injury and healing, trajectory values were scaled relative to uninjured tissue values (Figure 1G). Quantification revealed a more striking transcriptional shift from uninjured baseline in DTA compared with BT. After the initial injury, the regenerative P3 DTA showed a sharp restoration to near-uninjured conditions by 28 days after injury, whereas HO mesenchymal cells showed a more tempered restoration, remaining short of the uninjured state after day 42 after injury (Figure 1G).

To understand the early transcriptional changes that occur in response to the various injuries, we identified genes that showed differential expression across pseudotime (Figure 1) and subjected genes that showed enhanced expression in the early response phase to pathway analysis (Figure 2A). Several terms were found to enrich across multiple injury types, including shifts in bioenergetics (oxidative phosphorylation [OxPhos] and tricarboxylic acid cycle) and interactions between cells and their surroundings (ECM-receptor interaction, focal adhesion). To quantify levels of pathway activation, modular scores for selected KEGG terms were calculated. Modular scores represent the average expression of a defined gene list (Table S2) relative to random background. All injury types showed an increased bioenergetic need, enriching for genes linked to OxPhos (Figure 2A). Overlap analysis of genes specifically expressed in this early response to injury window

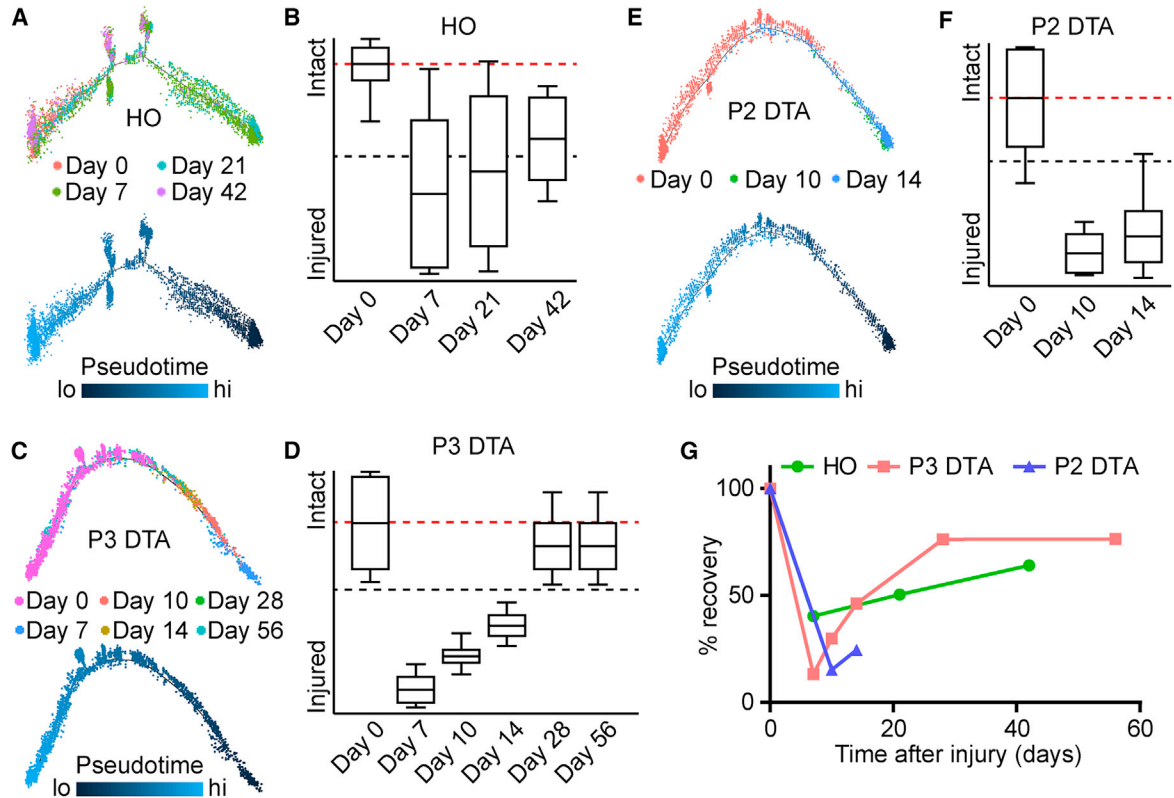


Figure 1. Trajectory analysis of mesenchymal cells shows a milder response to injury and slower recovery after BT

- (A) Trajectory analysis of mesenchymal-lineage cells from the injured Achilles tendon after BT.
 (B) Pseudotime analysis showing recovery after injury. A red dotted line denotes the average position of uninjured cells, and a black dotted line denotes the mid-point of the overall trajectory across all time points.
 (C) Trajectory analysis of fibroblast-like connective tissue cells in the regenerated region after P3 amputation.
 (D) Pseudotime analysis showing recovery after injury.
 (E) Trajectory analysis of fibroblast-like connective tissue cells in the regenerated region after P2 amputation.
 (F) Pseudotime analysis showing recovery after injury.
 (G) Normalized scoring of recovery after injury over time.
 The box (B, D, and F) represents 1 (lower), 2 (midline) and 3rd (upper) quartile values while the whiskers indicate standard deviation.

(highlighted in Figure 2A) showed substantial overlap between HO and P2 DTA injuries, whereas overlap between HO and P3 DTA as well as P3 and P2 DTA existed to a much lesser extent (Figure 2B; Table S1). Focusing on specific pathways activated early after injury, P2 DTA showed increased expression of ECM receptor interactors, whereas P3 DTA showed enrichment in terms such as chemokine signaling, nuclear factor κ B (NF- κ B), and hypoxia-related signaling (Figure 2C). These data suggests that, although some conservation between injury models exists, including an increased bioenergetic need and increased matrix interaction, these injury models showed altered levels of transcriptional activation, indicated by their distribution cells along their pseudotemporal axis, after injury in addition to injury-specific pathway enrichment.

Axolotl limb regeneration identifies mechanical response, WNT signaling, and inflammatory signaling as divergent properties of regenerative and fibrotic chondrogenesis

In contrast to P3 DTA, which regenerates through direct intramembranous ossification (Fernando et al., 2011), bone from the HO (Agarwal et al., 2016) and P2 DTA (Dawson et al., 2016) injury models forms through endochondral ossification via a cartilage intermediate. To better understand the biology of aberrant versus regenerative chondrogenesis, we next compared the transcriptional profile of the chondrogenic trajectory branches of mouse HO (Figures 3A and 3B) and connective tissue progenitor and differentiated cells from axolotl limb regeneration (Gerber et al., 2018; Figures 3C and 3D). Genes enriched in the chondrogenic branches from mouse HO and axolotl limb

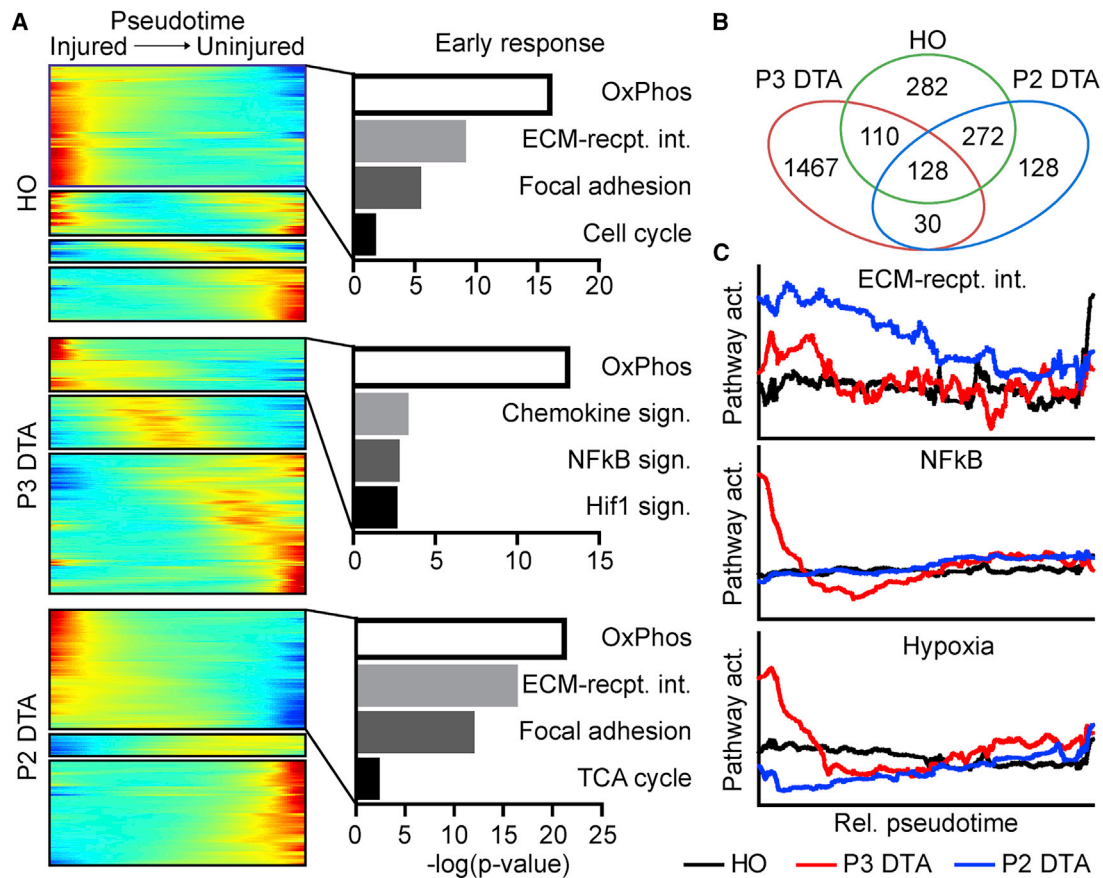


Figure 2. Common and alternative responses of reparative cells to early injury

(A) Pathway analysis of genes showing enriched expression in early pseudotime after injury.

(B) Venn diagram showing overlapping gene expression in the early stages after injury (identified in A).

(C) Pathway activation of transcripts linked to ECM-receptor interactions, NF-κB, and hypoxia across pseudotime.

regeneration (Figure 3E) were subjected to pathway analysis. As expected, several biological terms were co-enriched in the two datasets, including several terms linked to cartilage development and condensation, wound healing, and ossification (Figure 3F). However, several biological terms also diverged between the two models (Figure 3G). Although mouse HO chondrogenic cells were more enriched for terms linked to fibroblast growth factor (FGF) signaling and response to mechanical stimuli, axolotl chondrocytes instead showed enrichment in canonical and non-canonical WNT signaling as well as several inflammatory signaling cascades (Figure 3G). These data suggest that, although chondrogenesis in itself may not lead to aberrant repair, regenerative and fibrotic cartilage possess a unique transcriptional profile that may affect healing.

MPCs differ by fine-tuning ECM production/interaction and morphogenetic pathway activation

To understand the different fates of progenitor cells from each of the injuries, whole single-cell datasets from time

points critical for cell fate determination were combined, including HO day 7 (Sorkin et al., 2020; Pagani et al., 2021), P3 DTA day 10 (Storer et al., 2020)/11 (Johnson et al., 2020), and P2 DTA day 10 (Storer et al., 2020) (Figure 4A). Although derived from different tissues and consisting of progenitors with divergent differentiation potential, anchor-based analyses placed all mesenchymal cells in a single cluster, here called MPCs for simplicity. After identifying each cell cluster using marker gene expression (Figure 4B), pathway analysis was conducted on differentially expressed genes enriched in the cumulative MPC cluster relative to other cells present across all injury sites (Figure 4C). To confirm a specific regulation of identified KEGG pathways, modular scores were calculated (see Table S2 for gene lists). All MPCs across the injury types enriched for biological pathways linked to ECM organization and wound healing as well as transcriptional regulation of genes in the transforming growth factor β (TGF-β) and WNT signaling pathways compared with other cell types present in the repair environment (Figure 4D). MPCs shared a common

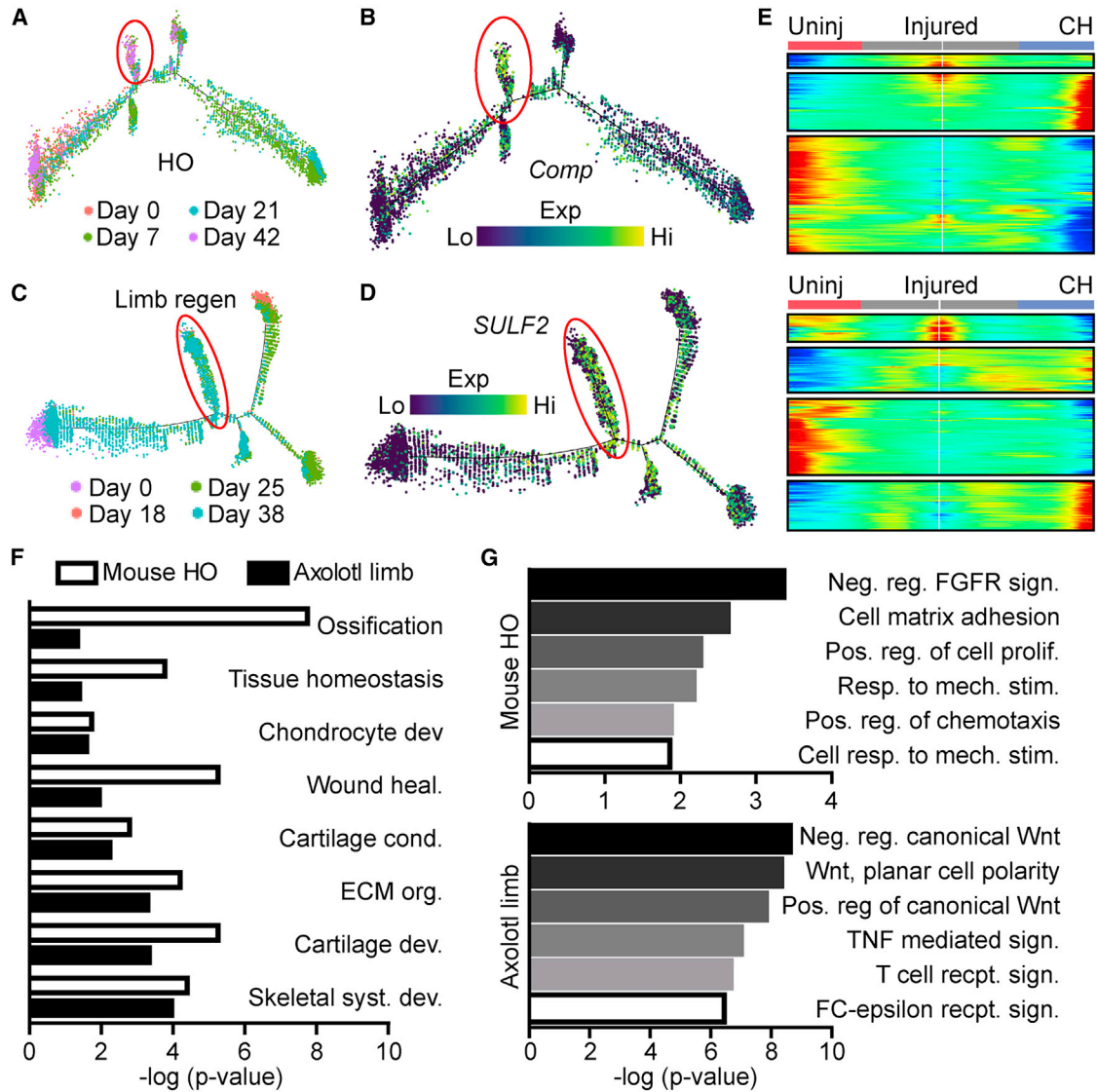


Figure 3. Comparison of chondrogenesis under fibrotic and regenerative conditions

- (A) Trajectory analysis of the mouse HO time course revealed a secondary branch enriched for late-stage cells.
 (B) Expression of the chondrogenic marker *Comp* in the chondrogenic branch of the HO dataset.
 (C) Trajectory analysis of connective tissue cells from the axolotl dataset after limb amputation, with the chondrogenic arm circled.
 (D) Expression of the chondrogenic marker *SULF2* in the chondrogenic branch of the axolotl dataset.
 (E) Branching analysis gene expression of chondrogenic arms from the mouse HO and axolotl limb amputation datasets.
 (F) Overlapping pathways enriched in the chondrogenic arms of both mouse HO and Axolotl limb.
 (G) Divergent pathways enriched in the chondrogenic arms of mouse HO or axolotl limb regeneration.

phenotype of being mass producers of matrix components, notably enriching in fibrillar collagen production and, to a lesser extent, ECM components and modifiers (Figure 4E; Table S4). These data suggest that, regardless of injury type, the function of MPCs is to begin the tissue repair process through deposition of new matrix components and that this process occurs through regulation of common morphogenetic pathways such as WNT and TGF- β .

Although many aspects of MPC biology were conserved across injury MPCs, we next sought to better understand what made each injury environment unique (Figure 5A). After normalizing for dataset depth and the relatively high number of HO cells in this merged dataset, cluster distribution showed slight enrichment (defined as a deviation from the expected one-third expectation) for neural-like cells and MPCs in the regenerative P3 DTA, whereas

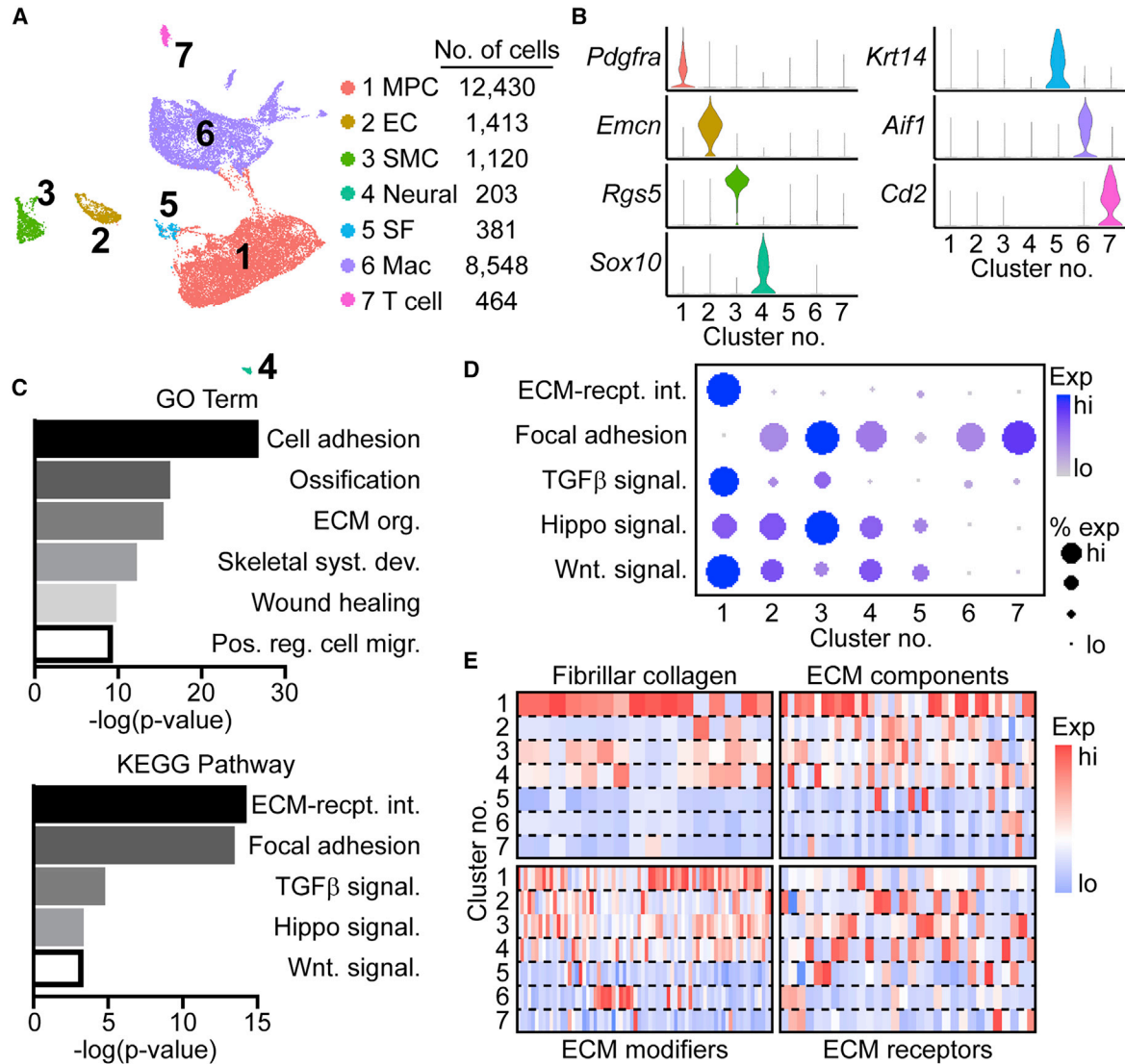


Figure 4. MPCs from various injury models show a common transcriptional response to facilitate injury repair/regeneration

(A) UMAP projection of all cells recovered after injury from models of heterotopic ossification (HO; day 7) or digit tip amputation (DTA) at P2 (day 10) or P3 (days 10–11).

(B) Violin plots showing marker gene expression used to identify mesenchymal progenitor cells (MPCs; *Pdgfra*), endothelial cells (ECs; *Emcn*), smooth muscle cells (SMCs; *Rgs5*), neural-derived cells (*Sox10*), skin fibroblasts (SFs; *Krt14*), macrophages (Macs; *Aif1*), or T cells (*Cd2*).

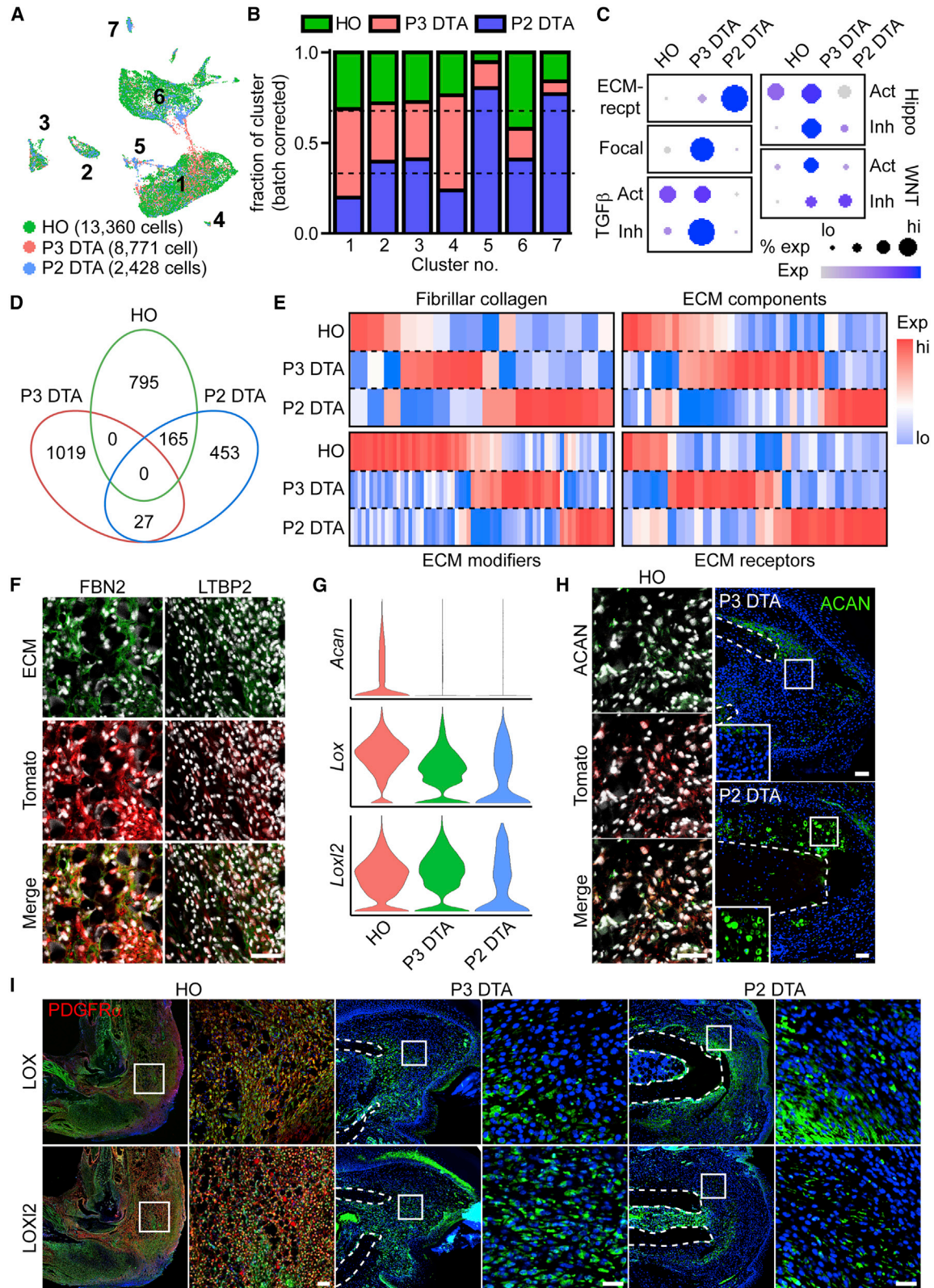
(C) GO term and KEGG gene enrichment analysis of DEGs in the MPC population.

(D) Module scoring of KEGG terms found to be differentially regulated in the MPC population.

(E) Heatmap expression of matrix components and interactors across clusters.

macrophages appeared to be overrepresented in the fibrotic HO and P2 DTA models. P2 DTA also showed strong enrichment in T cell recruitment in the injury environment in addition to high levels of skin fibroblasts, likely indicating an artifact of the surgical microdissection technique used for sample isolation (Figure 5B). Looking at the MPC-enriched pathways identified above, differential analyses suggest that, although these pathways may be conserved rela-

tive to other cell types in the injury environment, each pathway is fine-tuned in MPCs from each injury type (Figure 5C). HO MPCs showed high expression of TGF- β activators and minimal expression of pathway inhibitors likely driving previously observed chondrogenesis. In contrast, and consistent with regenerative chondrogenesis observed in axolotl limb regeneration, P3 DTA MPCs showed relatively strong activation of WNT signaling in addition to



(legend on next page)



relatively high expression of transcripts linked to assembly of focal adhesions relative to MPCs from other injury conditions. Comparatively, P2 DTA MPCs showed high levels of ECM interaction and Hippo pathway activation (Figure 5C). Focusing exclusively on the MPC cluster, differential gene expression revealed a large portion of uniquely regulated genes in the MPCs from each injury type. Differentially expressed genes (DEGs) revealed greater similarity between MPCs of the HO tendon and the P2 DTA and then between P3 and P2 DTA MPCs (Figure 5D; Table S3), reminiscent of the results in Figure 2B, which showed a more similar early response to injury between HO and P2 DTA. These data suggest that injury response and healing outcome, rather than injury type or anatomical site of origin, may be more prominent drivers of transcriptional changes. Although noted previously that MPCs are major matrix producers, each injury was associated with a unique set of matrix components (Figure 5E). HO was preferentially enriching for ECM modifiers, P3 DTA for ECM components, and P2 DTA for fibrillar collagens and ECM receptors. Production of matrix components linked previously to P3 DTA regeneration (Storer et al., 2020) were confirmed to be produced by MPCs in the HO site by staining the mesenchymal lineage mouse *Pdgfra-CreER;Rosa-tdTomato* with antibodies against FBN2 and LTBP2 (Figure 5F). To support our computational results, we specifically looked at the expression profiles of the ECM component ACAN and the ECM modifiers LOX and LOXL2 (Figure 5G). ACAN was found to be robustly expressed by MPCs in the HO, whereas relatively low levels were observed in the P3 DTA blastema (Figure 5H). P2 DTA showed production of ACAN in hypertrophic chondrocytes, identified by their large, round shape (Figure 5H), but these cells are poorly incorporated into single-cell droplets and were most likely absent/rarely abundant in the single-cell dataset. Consistent with gene expression analysis, immunofluorescence showed robust production of the ECM modifier LOX and,

to a lesser extent, LOXL2 in day 7 HO samples (Figure 5I). Inversely, day 10 P3 DTA blastema showed more widespread production of LOXL2, with LOX production more restricted to the proximal blastema region. Day 10 P2 DTA showed a similar staining profile as HO, with LOX produced at higher levels than LOXL2, although both ECM modifiers were present to a lesser extent than observed in HO. Overall, these results confirm that, although MPCs across all injury types share a common transcriptional profile related to matrix production and pathway modulation, these conserved pathways are fine tuned in each injury depending on the level of damage and the healing outcome.

Injury-specific inflammatory pathway activation in MPCs and immune cells are driven by altered cell-cell communication

Overall communication between cell types was evaluated in a pairwise fashion (Figure 6A), with line color indicating enrichment in the color-matched injury type labeled above and line thickness indicating the strength of change in overall signaling strength. Overall, HO showed the strongest predicted communication strength between MPCs (cluster 1) and macrophages (cluster 6) and T cells (cluster 7) compared with either DTA model. P2 DTA showed preferential MPC-macrophage signaling, whereas P3 DTA favored MPC-T cell signaling. In terms of immune cell-MPC signaling, P2 DTA showed the strongest communication between macrophages and MPCs, whereas HO showed the greatest strength in T cell-to-MPC signaling. Similar to MPC-to-immune cell communication, immune cell-to-MPC signaling was low in P3 DTA, with P2 DTA showing the strongest macrophage-MPC signaling, whereas HO showed the strongest T cell-MPC signaling. It is also interesting that, in comparison with MPC-immune cell crosstalk, P2 DTA MPCs showed the weakest self-signaling in the MPC cluster. To characterize shifts in immune cell populations affecting this MPC-immune cell crosstalk,

Figure 5. Differential analysis shows alternative activation of morphogenetic and ECM transcripts between injury types

- (A) UMAP projection of all cells recovered after injury from models of HO (day 7), or DTA at P2 (day 10) or P3 (days 10–11), colored by injury type.
- (B) Relative proportion of each cluster comprised of each injury type, corrected for batch size.
- (C) Module scoring of KEGG terms shown to be enriched in MPCs relative to other cell types in the injury environment.
- (D) DEGs in the MPCs between each of the 3 injuries.
- (E) Heatmap expression of matrix components and interactors in MPCs across injury types.
- (F) Immunofluorescence of ECM components (green), overlaid with *PDGFRa-CreER;Rosa-tdTomato* (red), shown previously to be expressed in the blastema.
- (G) Violin plots of select matrix components and modifiers.
- (H) Immunofluorescence of ACAN (green) in the HO (day 7), P3 DTA (day 10), and P2 DTA (day 10) injury models. HO images are overlaid with *PDGFRa-CreER;Rosa-tdTomato* (red) to identify the MPC population.
- (I) Immunofluorescence of the matrix modifiers LOX and LOXL2 (green) in the HO (day 7), P3 DTA (day 10), and P2 DTA (day 10) injury models. HO images are co-stained with *PDGFRα* (red) to identify the MPC population. Scale bars, 50 μm .

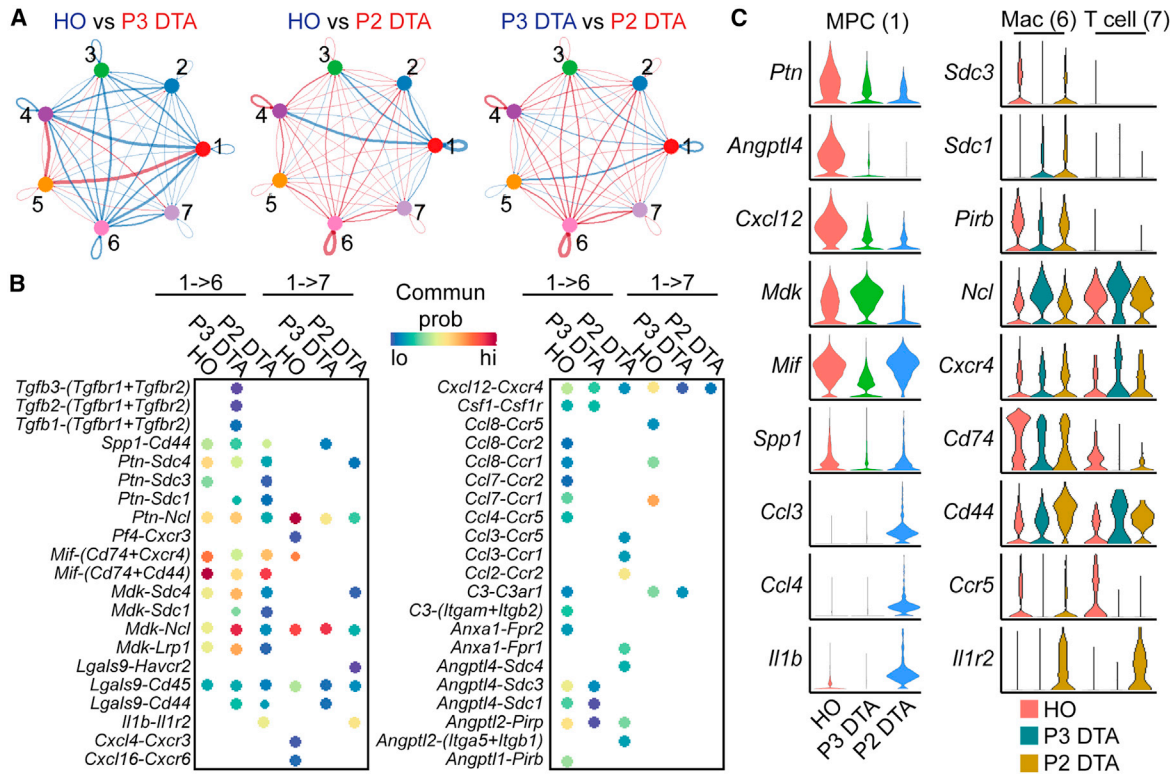


Figure 6. MPC-immune cell crosstalk after regenerative and fibrotic injuries

(A) Pairwise, strength-weighted interaction map between HO, P3 DTA, and P2 DTA, showing preferential signaling between each cluster from UMAP generated in Figure 4A. Line color denotes increased strength in the injury matching the color label above. The weight of a line denotes change in interaction strength, with thicker lines representing larger changes in interaction strength.

(B) Enriched ligand-receptor pairs used for MPC-to-immune cell communication.

(C) Violin plots showing differential expression of ligands in MPCs (left) and receptors in immune cell populations (right).

macrophages from the three injury models were analyzed (Figure S2). Although no significant differences were observed in average macrophage activation, HO and P3 DTA showed a significantly greater distribution in values, whereas P2 DTA macrophages were highly uniform (Figure S2A). Assessment of macrophage polarization showed HO and P2 DTA to be significantly biased toward a more polarized state, whereas P3 DTA macrophages significantly skewed toward a more non-polarized state (Figure S2B). Overall characterization indicated a high abundance of mature, polarized M1-like and M2-like macrophages in the HO site (Figure S2C). In comparison, P3 DTA showed a high prevalence of pre-activation and transitional macrophages, with P2 DTA showing an intermediate response with high levels of transitional and M1-like macrophages.

Focusing on MPC-to-immune cell communication, several predicted ligand-receptor pairs were identified to mediate this crosstalk (Figure 6B). Although several signaling networks were present to some extent across all injury environments (e.g., *Cxcl12-Cxcr4*), others showed a clear speci-

ficity for only some injury conditions (e.g., *Tgfb1-Tgfb1/2* between MPCs and macrophages was only present in P3 DTA). This was confirmed using violin plots, which show divergent expression of ligands and receptors across injury types (Figure 6C). These results included preferential expression of *Cxcl12* in HO MPCs, *Mif* in fibrotic HO and P2 DTA MPCs, and *Mdk* in the regenerative P3 DTA MPCs.

Conducting differential expression of predicted ligands between injury sites showed a consistent finding of injury-specific signaling (Figure 7A). Looking at predicted downstream signaling of the identified differentially expressed ligands (Figure 7B), pathway analysis showed alternative regulation of several prominent inflammatory pathways. Looking at overall activation of these pathways in MPCs and immune cells using module scoring (Table S2), we found a clear and distinct pattern of inflammatory pathway activation not only in immune cells but also in MPCs themselves (Figure 7C). P2 DTA showed high levels of inflammatory pathway activation in immune cells, but only Toll-like receptor signaling appeared to be enriched in the MPCs. In contrast, P3 DTA showed relatively high levels of

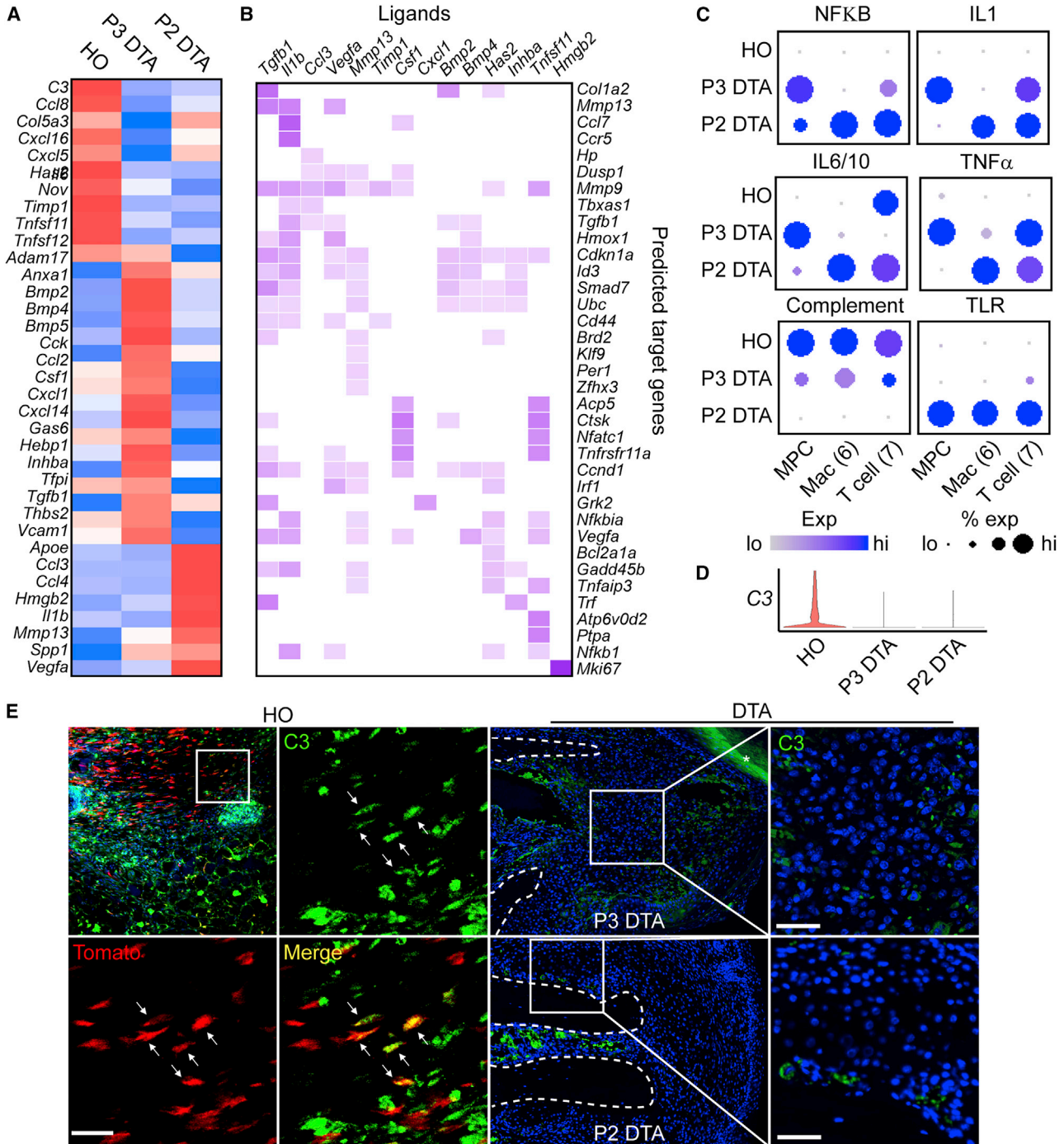


Figure 7. MPCs show differential activation of inflammatory cascades after injury

(A) Differentially enriched ligands derived from MPC clusters.

(B) Comparison of ligands and predicted downstream targets alternatively expressed in HO versus DTA (P3).

(C) Inflammatory pathway module scoring in MPCs, Macs, and T cells. Dots are scaled individually between clusters.

(D) Violin plot showing expression of *C3* in HO, P3 DTA, and P2 DTA MPCs.

(E) Immunofluorescence imaging of *C3* in HO, P3 DTA, and P2 DTA mouse models.

HO images are overlaid with *PDGFRa-CreER;Rosa-tdTomato* (red) to identify the MPC population. Scale bars, 50 μ m.



inflammatory pathway activation in the MPCs, including NF- κ B, interleukin-1 (IL-1), IL-6/10, and tumor necrosis factor alpha (TNF- α) (Figure 7C). Although inflammation is a major instigator, only the classic complement pathway was enriched in HO compared with the DTA models. To validate this increased complement activation, we analyzed the complement component C3 in HO, P3 DTA, and P2 DTA models. In our single-cell datasets, C3 was found to be primarily expressed in HO MPCs (Figure 7D). This preferential enrichment in HO was confirmed using immunofluorescent staining, which showed robust labeling of C3 throughout the HO site, including *Pdgfra-CreER;tdTomato*-positive MPCs (Figure 7E). In comparison, minimal C3 staining was detected in the fibroblasts 10 days after P3 or P2 DTA. These data suggest that outcomes between regenerative P3 DTA and fibrotic HO and P2 DTA models differ not only at the MPC level but also in the overall cellular crosstalk in the injury site and that the inflammation may differentially and directly affect MPC fate and function in each injury environment.

DISCUSSION

In this study, we present data delineating the response after injury and how changes in the injury environment dictate regenerative or fibrotic healing. Our data indicate a common trajectory of cells in the injury site to return to an uninjured transcriptional state, regulating common cell functions such as bioenergetics and interactions with the ECM and/or other cells. Focusing on the critical phase of cell fate determination, MPCs showed unique responses to major morphogens such as TGF- β and WNTs and were the major producers of most matrix components. Although commonly enriched in MPCs across all injuries, the extent of morphogenetic pathway activation and matrix production is tightly titrated between the different injury types. Even when analyzing the differences in MPC clusters, P2 DTA MPCs have more in common transcriptionally with HO MPCs than MPCs derived from the neighboring P3 amputation. These data support the notion that, although each of the various injuries include a unique set of progenitor cells pre-disposed toward differentiation toward certain lineages (e.g., chondrocytes, osteoblasts, tenocytes, etc.), outcome rather than anatomical site is a larger determinant of transcriptional response at this critical healing stage. Finally, we show that these transcriptional differences in MPCs of HO and P2 and P3 DTA extend to the inflammatory nature of the injury, not only in the mesenchymal-to-immune cell crosstalk but also activation of inflammatory pathways in the MPCs themselves.

Following injury, trajectory analyses demonstrated a strong transcriptional response in MPCs, consistent with

a dramatic change to the injury environment. In comparison with the steep and coordinated response to injury observed in the DTA model, BT resulted in a more modest transcriptional change. The reduced severity may reflect the fact that a single tendon injury is less severe than the severing of bone, skin, nail, and connective tissue occurring in the DTA model. Although the overall injury may be less severe, HO MPCs showed a wide variation in transcriptional response. This variation may be in part due to the fact that no healthy tissue resides in the regenerated region of the DTA models, whereas analysis of the HO site is likely to include uninjured tendon tissue. Signaling cues are likely derived from several sources in the HO model, including the underlying periosteum and the neighboring severed tendon ends, whereas the DTA model likely represents a more uniform signaling gradient derived from the bone stump/nail bed and, later, the closing wound epidermis. Therefore, it will be of keen future interest to understand the contribution of each of these surrounding tissues to the overall signaling in the healing environment and how these microdomains may contribute to cell fate in each of the injury models.

Next we sought to compare the genetic profiles of MPCs involved in DTA repair and HO formation at the critical stages of cell fate determination. These analyses demonstrate that, although derived from different tissue regions, MPCs from each of the injury site have common characteristics of high ECM interaction, upregulation of morphogen-mediated signaling, and striking production of reparative ECM components. MPCs from each injury type showed a unique ECM profile, with HO MPCs heavily expressing ECM modifiers, P3 DTA MPCs producing more ECM components, and P2 DTA producing more fibrillar collagens and ECM receptors. Although the intramembranous nature of P3 DTA formation may partially explain some of these differences, the strong divergence in matrix production between the endochondral HO and P2 DTA injuries suggests that more work is needed to understand how these differential matrix constituents may contribute to healing outcomes. Probing for expression of several matrix components that are critical for DTA repair (Storer et al., 2020), we found that HO MPCs produced FBN2 and LTBP2 during ectopic bone formation. Previous sequencing results have also shown these same matrix components as being upregulated after femur fracture in the mouse, suggesting that these markers may be broadly important for bone wound repair (Coates et al., 2019).

Finally, we show that the crosstalk between progenitors and immune cells is highly altered in the different injury regions. Macrophages have known critical roles in injury healing, including in P3 DTA and HO injuries. Analyses of macrophages across the 3 injuries showed a high prevalence of mature, polarized macrophages with the HO site,



consistent with a highly inflammation-driven process (Sorokin et al., 2020). In contrast, macrophages in the P3 DTA were present in a more pre-activation or transitional state, consistent with a more controlled, pro-regenerative inflammatory environment (Simkin et al., 2017). Our data suggest a stronger interaction between MPCs and immune cells in our fibrotic healing models relative to the regenerative P3 DTA injury. Interaction studies identified injury, fibrotic, and regeneration-specific MPC-derived factors through which this MPC-immune cell crosstalk was executed. CXCL12 is a known recruiter of *Cxcr4*-expressing immune cells and was found to be robustly expressed in the MPCs at the site of HO. This high expression likely contributes to the strong and prolonged levels of inflammation in the BT injury site, necessary for HO formation. In contrast to HO, P2 DTA MPCs showed enriched expression of *Il1b*. Although IL-1 β is typically thought of as a pro-inflammatory cytokine produced by macrophages, IL-1 signaling has also been shown to induce innate inflammation (Dinarello 2018), potentially contributing not only to the aberrant healing in P2 DTA but also to the increased prevalence of T cells in this injury model. Although sharing several injury-specific crosstalk mechanisms, commonalities were also observed across fibrotic injury models, including increased expression of *Mif*. *Mif* expression has been linked to inflammatory disorders such as sepsis as well as organ pathologies such as fibrosis (Jankauskas et al., 2019), with *Mif*-mediated signaling in macrophages associated with polarization of M0 or M2 subtypes into their more pro-inflammatory M1 state (Figueiredo et al., 2018). In contrast to the more pro-inflammatory markers, MPCs derived from a P3 DTA injury showed elevated signaling via *Mdk*. MDK signaling through macrophage LRP1 helps attenuate pro-inflammatory macrophage activation (Mantuano et al., 2016), whereas signaling through NCL may help macrophages recognize apoptotic cells (Hirano et al., 2005). One limitation of these analyses is the fact that, although these cell types may indeed have the ability to communicate, their proximity may be insufficient for this crosstalk to occur. Spatial validation is required to discriminate which of these predicted pathways have a functional role in each of the injury conditions. However, these data suggests that, although immune cell activation and recruitment are essential for overall healing across injury models, crosstalk between MPCs and these recruited immune cells can drastically alter the overall inflammatory status of the injury environment, likely contributing to overall healing outcomes.

In addition to inflammatory immune cells, our data suggest that activation of key inflammatory pathways may also play a direct role in cell fate outcomes of MPCs in the injury environments. HO MPCs showed enriched expression of genes linked to the classic complement

pathway as well as increased production of the complement component C3. Although the complete function of this pathway remains to be determined, complement activation in dental pulp has been shown to help initiate regeneration (Chmilewsky et al., 2014), with specific complement components such as C1q also connected to activation of DDR2 (Hayuningtyas et al., 2021), potentially regulating downstream mechanotransduction, recently demonstrated to be critical in bone formation in the HO (Huber et al., 2020) and P3 DTA injury models (Dolan et al., 2021). In contrast, the P2 DTA MPCs showed preferential activation of Toll-like receptor (TLR) signaling, which has been linked previously to overall organ fibrosis (Huebener and Schwabe 2013), including persisting fibrosis in scleroderma (Bhattacharyya et al., 2017). The importance of these inflammatory pathway activations occurring in MPCs is highlighted by our comparison of endochondral bone healing mediated in mouse HO compared with the gold standard of regeneration in the axolotl. These comparisons revealed that, although HO and limb regeneration showed common activation of wound healing, chondrogenic differentiation, and skeletal morphogenesis, axolotl chondrocytes also enriched for genes in typical inflammatory networks. This mirrored activation of inflammatory pathways in the early P3 DTA response, suggesting that modulation of these pathways in the MPCs may hold significant sway in modulating more favorable outcomes. In comparison with the fibrotic injuries, regenerative P3 DTA MPCs showed preferential activation of inflammatory pathways such as NF- κ B and IL-1 in the MPCs. Previous studies have suggested a role of NF- κ B in proliferation of synoviocytes in rheumatoid arthritis (Samimi et al., 2020), and reducing expression of canonical NF- κ B has been linked to differentiation of muscle (Canicio et al., 2001) and embryonic stem cells (Armstrong et al., 2006; Deng et al., 2019). Similarly, IL-1 signaling has been shown to promote hematopoietic progenitor cell proliferation and cell survival (Orelino et al., 2009) and drive early stages of cardiac fibroblast remodeling after infarction (Bageghni et al., 2019).

Our data suggest that, although MPCs derived from different injuries may share a common early response, ECM deposition, interaction, and morphogen signaling is finely tuned in an outcome-specific fashion to determine healing mechanisms. This fine tuning is extended to crosstalk between MPCs and cells of the immune system. Response to inflammation through immune cell interaction or direct regulation of MPCs refines signaling cascades to determine the type and extent of the repair response. Understanding these signals could help enhance healing under conditions of repair or regeneration while controlling or preventing ectopic or aberrant tissue formation.



EXPERIMENTAL PROCEDURES

Additional details regarding animal models, computational analyses, antibody staining, and data availability can be found in the [supplemental data](#).

Trajectory analysis

MPCs from HO, P3 DTA, and P2 DTA were isolated based on marker expression and subjected to trajectory analysis using the R package Monocle. Root states were manually determined based on enriched abundance of cells at time points taken shortly after injury. Pseudotime values were then assigned and individually scaled within each injury type according to the lowest (0%) and highest (100%) pseudotime value to represent percent recovery. Next, genes that showed a correlative expression with pseudotime values were calculated and grouped into the minimum number of clusters to identify genes preferentially expressed in the early injury phase only. For chondrogenic analysis, trajectory states enriched for chondrogenic markers were selected for branched expression analysis modeling (BEAM). As above, genes were clustered at the minimum level needed to identify genes enriched in the chondrogenic state.

Pathway analyses

All pathway analyses were conducted using the Database for Annotation, Visualization, and Integrated Discovery (DAVID) (Huang et al., 2009) using significantly regulated genes. To quantify pathway activation, curated gene lists were assembled from KEGG pathways (Table S2) and quantified using the AddModuleScore function of Seurat (Stuart et al., 2019). Overall pathway activation was defined as the modular score for activation minus the modular score for inhibition.

Interaction analysis

Pairwise, strength-weighted interaction analyses were conducted using the R package CellChat (Jin et al., 2021). Predictive ligand-receptor pairs were identified by individually analyzing each injury dataset separately. To determine differentially expressed ligands, receptors, and downstream targets, the R package NicheNet (Browaeys et al. 2020) was used.

SUPPLEMENTAL INFORMATION

Supplemental information can be found online at <https://doi.org/10.1016/j.stemcr.2022.08.011>.

ACKNOWLEDGMENTS

The authors wish to acknowledge K. Kessell and the University of Michigan Unit for Laboratory Animal Medicine for excellent animal care. N.J.E. was supported by a Ruth L. Kirschstein Institutional National Research Service Award postdoctoral fellowship (T32-HD007505). Work was supported by R01AR071379 and R01AR078324 from the National Institutes of Health (NIH) to B.L. and US Department of Defense Grant and W81XWH-19-PROP-ARA (OR190048) (to B.L.). The funders had no role in study design, data collection and analysis, decision to publish, or preparation of the manuscript.

AUTHOR CONTRIBUTIONS

Conception or design of the work, R.J.T. and B.L.; data collection, R.J.T., A.C.B., S.B., N.J.E., C.A.P., and L.A.D.; data analysis and interpretation, R.J.T., A.R.C., S.B., and L.A.D.; drafting the article, R.J.T.; critical revision of the article, B.L. All authors approved the final version of the manuscript.

CONFLICT OF INTERESTS

The authors declare no competing interests.

Received: March 16, 2022

Revised: August 25, 2022

Accepted: August 25, 2022

Published: October 11, 2022

REFERENCES

- Agarwal, S., Loder, S., Brownley, C., Cholok, D., Mangiavini, L., Li, J., Breuler, C., Sung, H.H., Li, S., Ranganathan, K., et al. (2016). Inhibition of Hif1alpha prevents both trauma-induced and genetic heterotopic ossification. *Proc. Natl. Acad. Sci. USA* *113*, E338–E347.
- Armstrong, L., Hughes, O., Yung, S., Hyslop, L., Stewart, R., Wappler, I., Peters, H., Walter, T., Stojkovic, P., Evans, J., et al. (2006). The role of PI3K/AKT, MAPK/ERK and NF kappa beta signalling in the maintenance of human embryonic stem cell pluripotency and viability highlighted by transcriptional profiling and functional analysis. *Hum. Mol. Genet.* *15*, 1894–1913.
- Aztekin, C., Hiscock, T.W., Marioni, J.C., Gurdon, J.B., Simons, B.D., and Jullien, J. (2019). Identification of a regeneration-organizing cell in the *Xenopus* tail. *Science* *364*, 653–658.
- Bageghni, S.A., Hemmings, K.E., Yuldasheva, N.Y., Maqbool, A., Gamboa-Esteves, F.O., Humphreys, N.E., Jackson, M.S., Denton, C.P., Francis, S., Porter, K.E., et al. (2019). Fibroblast-specific deletion of interleukin-1 receptor-1 reduces adverse cardiac remodeling following myocardial infarction. *JCI Insight* *5*, 125074.
- Baker, C.E., Moore-Lotridge, S.N., Hysong, A.A., Posey, S.L., Robinette, J.P., Blum, D.M., Benvenuti, M.A., Cole, H.A., Egawa, S., Okawa, A., et al. (2018). Bone fracture acute phase response-A unifying theory of fracture repair: clinical and scientific implications. *Clin. Rev. Bone Miner. Metab.* *16*, 142–158.
- Beck, C.W., Christen, B., and Slack, J.M.W. (2003). Molecular pathways needed for regeneration of spinal cord and muscle in a vertebrate. *Dev. Cell* *5*, 429–439.
- Beck, C.W., Izpisua Belmonte, J.C., and Christen, B. (2009). Beyond early development: *Xenopus* as an emerging model for the study of regenerative mechanisms. *Dev. Dyn.* *238*, 1226–1248.
- Bhattacharyya, S., Midwood, K.S., Yin, H., and Varga, J. (2017). Toll-like receptor-4 signaling drives persistent fibroblast activation and prevents fibrosis resolution in scleroderma. *Adv. Wound Care* *6*, 356–369.
- Browaeys, R., Saelens, W., and Saey, Y. (2020). NicheNet: modeling intercellular communication by linking ligands to target genes. *Nat. Methods* *17*, 159–162.



- Canicio, J., Ruiz-Lozano, P., Carrasco, M., Palacin, M., Chien, K., Zorzano, A., and Kaliman, P. (2001). Nuclear factor kappa B-inducing kinase and I kappa B kinase-alpha signal skeletal muscle cell differentiation. *J. Biol. Chem.* *276*, 20228–20233.
- Carr, M.J., Toma, J.S., Johnston, A.P.W., Steadman, P.E., Yuzwa, S.A., Mahmud, N., Frankland, P.W., Kaplan, D.R., and Miller, F.D. (2019). Mesenchymal precursor cells in adult nerves contribute to mammalian tissue repair and regeneration. *Cell Stem Cell* *24*, 240–256.e9.
- Chmielewsky, F., Jeanneau, C., Laurent, P., and About, I. (2014). Pulp fibroblasts synthesize functional complement proteins involved in initiating dentin-pulp regeneration. *Am. J. Pathol.* *184*, 1991–2000.
- Coates, B.A., McKenzie, J.A., Buettmann, E.G., Liu, X., Gontarz, P.M., Zhang, B., and Silva, M.J. (2019). Transcriptional profiling of intramembranous and endochondral ossification after fracture in mice. *Bone* *127*, 577–591.
- Dawson, L.A., Simkin, J., Sauque, M., Pela, M., Palkowski, T., and Muneoka, K. (2016). Analogous cellular contribution and healing mechanisms following digit amputation and phalangeal fracture in mice. *Regeneration* *3*, 39–51.
- Dawson, L.A., Yu, L., Yan, M., Marrero, L., Schanes, P.P., Dolan, C., Pela, M., Petersen, B., Han, M., and Muneoka, K. (2017). The periosteal requirement and temporal dynamics of BMP2-induced middle phalanx regeneration in the adult mouse. *Regeneration* *4*, 140–150.
- Deng, P., Zhou, C., Alvarez, R., Hong, C., and Wang, C.Y. (2019). Inhibition of IKK/NF-kappa B signaling enhances differentiation of mesenchymal stromal cells from human embryonic stem cells (vol 6, pg 456, 2016). *Stem Cell Rep.* *12*, 180–181.
- Dinarello, C.A. (2018). Overview of the IL-1 family in innate inflammation and acquired immunity. *Immunol. Rev.* *281*, 8–27.
- Dolan, C.P., Imholt, F., Yang, T.J., Bokhari, R., Gregory, J., Yan, M., Qureshi, O., Zimmel, K., Sherman, K.M., Falck, A., et al. (2022). Mouse digit tip regeneration is mechanical load dependent. *J. Bone Miner. Res.* *37*, 312–322.
- Douglas, B.S. (1972). Conservative management of guillotine amputation of the finger in children. *Aust. Paediatr. J.* *8*, 86–89.
- Fernando, W.A., Leininger, E., Simkin, J., Li, N., Malcom, C.A., Sathyamoorthi, S., Han, M., and Muneoka, K. (2011). Wound healing and blastema formation in regenerating digit tips of adult mice. *Dev. Biol.* *350*, 301–310.
- Figueiredo, C.R., Azevedo, R.A., Mousdell, S., Resende-Lara, P.T., Ireland, L., Santos, A., Girola, N., Cunha, R.L.O.R., Schmid, M.C., Polonelli, L., et al. (2018). Blockade of MIF-CD74 signalling on macrophages and dendritic cells restores the antitumour immune response against metastatic melanoma. *Front. Immunol.* *9*, 1132.
- Gerber, T., Murawala, P., Knapp, D., Masselink, W., Schuez, M., Hermann, S., Gac-Santel, M., Nowoshilow, S., Kageyama, J., Khattak, S., et al. (2018). Single-cell analysis uncovers convergence of cell identities during axolotl limb regeneration. *Science* *362*, eaa0681.
- Han, M., Yang, X., Lee, J., Allan, C.H., and Muneoka, K. (2008). Development and regeneration of the neonatal digit tip in mice. *Dev. Biol.* *315*, 125–135.
- Hayuningtyas, R.A., Han, M., Choi, S., Kwak, M.S., Park, I.H., Lee, J.H., Choi, J.E., Kim, D.K., Son, M., and Shin, J.S. (2021). The collagen structure of C1q induces wound healing by engaging discoidin domain receptor 2. *Mol. Med.* *27*, 125.
- Hirano, K., Miki, Y., Hirai, Y., Sato, R., Itoh, T., Hayashi, A., Yamana, M., Eda, S., and Beppu, M. (2005). A multifunctional shuttling protein nucleolin is a macrophage receptor for apoptotic cells. *J. Biol. Chem.* *280*, 39284–39293.
- Huang, D.W., Sherman, B.T., and Lempicki, R.A. (2009). Systematic and integrative analysis of large gene lists using DAVID bioinformatics resources. *Nat. Protoc.* *4*, 44–57.
- Huber, A.K., Patel, N., Pagani, C.A., Marini, S., Padmanabhan, K.R., Matera, D.L., Said, M., Hwang, C., Hsu, G.C.Y., Poli, A.A., et al. (2020). Immobilization after injury alters extracellular matrix and stem cell fate. *J. Clin. Invest.* *130*, 5444–5460.
- Huebener, P., and Schwabe, R.F. (2013). Regulation of wound healing and organ fibrosis by toll-like receptors. *Biochim. Biophys. Acta* *1832*, 1005–1017.
- Illingworth, C.M. (1974). Trapped fingers and amputated finger tips in children. *J. Pediatr. Surg.* *9*, 853–858.
- Jin, S., Guerrero-Juarez, C.F., Zhang, L., Chang, I., Ramos, R., Kuan, C.H., Myung, P., Plikus, M.V., and Nie, Q. (2021). Inference and analysis of cell-cell communication using CellChat. *Nat. Commun.* *12*, 1088.
- Joe, A.W.B., Yi, L., Natarajan, A., Le Grand, F., So, L., Wang, J., Rudnicki, M.A., and Rossi, F.M.V. (2010). Muscle injury activates resident fibro/adipogenic progenitors that facilitate myogenesis. *Nat. Cell Biol.* *12*, 153–163.
- Johnston, A.P.W., Yuzwa, S.A., Carr, M.J., Mahmud, N., Storer, M.A., Krause, M.P., Jones, K., Paul, S., Kaplan, D.R., and Miller, F.D. (2016). Dedifferentiated schwann cell precursors secreting paracrine factors are required for regeneration of the mammalian digit tip. *Cell Stem Cell* *19*, 433–448.
- Kakebeen, A.D., Chitsazan, A.D., Williams, M.C., Saunders, L.M., and Wills, A.E. (2020). Chromatin accessibility dynamics and single cell RNA-Seq reveal new regulators of regeneration in neural progenitors. *Elife* *9*, e52648.
- Kikuchi, A., and Monga, S.P. (2015). PDGFRalpha in liver pathophysiology: emerging roles in development, regeneration, fibrosis, and cancer. *Gene Expr.* *16*, 109–127.
- Kikuchi, A., Singh, S., Poddar, M., Nakao, T., Schmidt, H.M., Gayden, J.D., Sato, T., Arteeel, G.E., and Monga, S.P. (2020). Hepatic stellate cell-specific platelet-derived growth factor receptor-alpha loss reduces fibrosis and promotes repair after hepatocellular injury. *Am. J. Pathol.* *190*, 2080–2094.
- Jankauskas, S.S., Wong, D.W.L., Bucala, R., Djudaj, S., and Boor, P. (2019). Evolving complexity of MIF signaling. *Cell. Signal.* *57*, 76–88.
- Johnson, G.L., Masias, E.J., and Lehoczy, J.A. (2020). Cellular heterogeneity and lineage restriction during mouse digit tip regeneration at single-cell resolution. *Dev. Cell* *52*, 525–540.e5.
- Lehoczy, J.A., Robert, B., and Tabin, C.J. (2011). Mouse digit tip regeneration is mediated by fate-restricted progenitor cells. *Proc. Natl. Acad. Sci. USA* *108*, 20609–20614.



- Mantuano, E., Brifault, C., Lam, M.S., Azmoon, P., Gilder, A.S., and Gonias, S.L. (2016). LDL receptor-related protein-1 regulates NF κ B and microRNA-155 in macrophages to control the inflammatory response. *Proc. Natl. Acad. Sci. USA* *113*, 1369–1374.
- Meyers, C., Lisiecki, J., Miller, S., Levin, A., Fayad, L., Ding, C., Sono, T., McCarthy, E., Levi, B., and James, A.W. (2019). Heterotopic ossification: a comprehensive review. *JBMR Plus* *3*, e10172.
- Nacu, E., and Tanaka, E.M. (2011). Limb regeneration: a new development? *Annu. Rev. Cell Dev. Biol.* *27*, 409–440.
- Neff, E.P. (2018). Dedifferentiation for regeneration. *Lab Anim.* *47*, 309.
- Neufeld, D.A., and Zhao, W. (1995). Bone regrowth after digit tip amputation in mice is equivalent in adults and neonates. *Wound Repair Regen.* *3*, 461–466.
- Olson, L.E., and Soriano, P. (2009). Increased PDGFR α activation disrupts connective tissue development and drives systemic fibrosis. *Dev. Cell* *16*, 303–313.
- Orelia, C., Peeters, M., Haak, E., van der Horn, K., and Dzierzak, E. (2009). Interleukin-1 regulates hematopoietic progenitor and stem cells in the midgestation mouse fetal liver. *Haematologica* *94*, 462–469.
- Pagani, C.A., Huber, A.K., Hwang, C., Marini, S., Padmanabhan, K., Livingston, N., Nunez, J., Sun, Y., Edwards, N., Cheng, Y.H., et al. (2021). Novel lineage-tracing system to identify site-specific ectopic bone precursor cells. *Stem Cell Rep.* *16*, 626–640.
- Roberts, S.J., van Gestel, N., Carmeliet, G., and Luyten, F.P. (2015). Uncovering the periosteum for skeletal regeneration: the stem cell that lies beneath. *Bone* *70*, 10–18.
- Nejabatbakhsh Samimi, L., Farhadi, E., Tahmasebi, M.N., Jamshidi, A., Sharafat Vaziri, A., and Mahmoudi, M. (2020). NF-kappa B signaling in rheumatoid arthritis with focus on fibroblast-like synoviocytes. *Autoimmun. Highlights* *11*.
- Simkin, J., Han, M., Yu, L., Yan, M., and Muneoka, K. (2013). The mouse digit tip: from wound healing to regeneration. *Methods Mol. Biol.* *1037*, 419–435.
- Simkin, J., Sammarco, M.C., Marrero, L., Dawson, L.A., Yan, M., Tucker, C., Cammack, A., and Muneoka, K. (2017). Macrophages are required to coordinate mouse digit tip regeneration. *Development* *144*, 3907–3916.
- Sorkin, M., Huber, A.K., Hwang, C., Carson, W.F., 4th, Menon, R., Li, J., Vasquez, K., Pagani, C., Patel, N., Li, S., et al. (2020). Regulation of heterotopic ossification by monocytes in a mouse model of aberrant wound healing. *Nat. Commun.* *11*, 722.
- Sousa, S., Afonso, N., Bensimon-Brito, A., Fonseca, M., Simões, M., Leon, J., Roehl, H., Cancela, M.L., and Jacinto, A. (2011). Differentiated skeletal cells contribute to blastema formation during zebrafish fin regeneration. *Development* *138*, 3897–3905.
- Storer, M.A., Mahmud, N., Karamboulas, K., Borrett, M.J., Yuzwa, S.A., Gont, A., Androschuk, A., Sefton, M.V., Kaplan, D.R., and Miller, F.D. (2020). Acquisition of a unique mesenchymal precursor-like blastema state underlies successful adult mammalian digit tip regeneration. *Dev. Cell* *52*, 509–524.e9.
- Stuart, T., Butler, A., Hoffman, P., Hafemeister, C., Papalexi, E., Mauck, W.M., 3rd, Hao, Y., Stoekius, M., Smibert, P., and Satija, R. (2019). Comprehensive integration of single-cell data. *Cell* *177*, 1888–1902.e21.
- Tanaka, H.V., Ng, N.C.Y., Yang Yu, Z., Casco-Robles, M.M., Maruo, E., Tsonis, P.A., and Chiba, C. (2016). A developmentally regulated switch from stem cells to dedifferentiation for limb muscle regeneration in newts. *Nat. Commun.* *7*, 11069.
- Uezumi, A., Fukada, S.i., Yamamoto, N., Takeda, S., and Tsuchida, K. (2010). Mesenchymal progenitors distinct from satellite cells contribute to ectopic fat cell formation in skeletal muscle. *Nat. Cell Biol.* *12*, 143–152.
- Uezumi, A., Ito, T., Morikawa, D., Shimizu, N., Yoneda, T., Segawa, M., Yamaguchi, M., Ogawa, R., Matev, M.M., Miyagoe-Suzuki, Y., et al. (2011). Fibrosis and adipogenesis originate from a common mesenchymal progenitor in skeletal muscle. *J. Cell Sci.* *124*, 3654–3664.
- Wosczyzna, M.N., Konishi, C.T., Perez Carbajal, E.E., Wang, T.T., Walsh, R.A., Gan, Q., Wagner, M.W., and Rando, T.A. (2019). Mesenchymal stromal cells are required for regeneration and homeostatic maintenance of skeletal muscle. *Cell Rep.* *27*, 2029–2035.e5.